Effect of NH 3 Adsorption on the Structural and Vibrational Properties of TS1

ARTICLE *in* THE JOURNAL OF PHYSICAL CHEMISTRY B · AUGUST 2002

Impact Factor: 3.3 · DOI: 10.1021/jp0257698

6 AUTHORS, INCLUDING:

Gabriele Ricchiardi
Università degli Studi di Torino
89 PUBLICATIONS **4,314** CITATIONS
SEE PROFILE

A. Zecchina
Università degli Studi di Torino
560 PUBLICATIONS **19,933** CITATIONS
SEE PROFILE

Carlo Lamberti
Università degli Studi di Torino
379 PUBLICATIONS **13,123** CITATIONS
SEE PROFILE

Effect of NH_3 Adsorption on the Structural and Vibrational Properties of TS-1

Alessandro Damin, Francesca Bonino, Gabriele Ricchiardi, Silvia Bordiga, Adriano Zecchina, and Carlo Lamberti*

Department of Inorganic, Physical and Material Chemistry, University of Turin, Via P. Giuria 7, I-10125 Torino Italy, and INFM UdR di Torino Università

Received: March 15, 2002; In Final Form: May 6, 2002

The major structural and vibrational features of TS-1 catalyst have been investigated by means of computational methods based on cluster/embedded cluster approach (ONIOM scheme). This approach has been able to reproduce the perturbation induced on the main structural and vibrational features by NH_3 adsorption.

Introduction

Ti-silicalite-1 (TS-1)[1] is an active and selective catalyst in a number of low-temperature oxidation reactions with aqueous H_2O_2 as the oxidant.[2] For its relevance in industrial applications, it has been one of the most studied materials in heterogeneous catalysis in recent years.[3−14] With respect to the Ti-free silicalite, TS-1 is characterized by an increase of the unit cell volume proportional to the Ti content[1,4−6] and by the presence of a peculiar IR absorption component[1,9−11,14] centered at 960 cm^{-1}. This band is well visible in the IR spectra since appearing in the low energy tail of the very strong absorption due to ν(Si−O−Si) modes appearing in the broad 1250−1030 cm^{-1} interval (vide infra Figure 1). In addition to the 960 cm^{-1} component, Raman experiments[10] have successively revealed the presence of a new fingerprint band at 1125 cm^{-1}, not visible in IR spectra. Li et al.[13] have recently demonstrated that only the latter undergoes a remarkable resonant enhancement upon using an exciting laser at $\lambda = 244$ nm, i.e., in the low energy tail of the $O^{2-}Ti^{4+} \rightarrow O^{-}Ti^{3+}$ ligand-to-metal charge-transfer transition.[9,11,14] The explanation of this different behavior has been discussed by us combining ab initio methods and spectroscopic experiments.[14] In that work the calculations have been limited to the simulation of TS-1 and silicalite in vacuum conditions using, as model, the $[Ti(OSi(OH)_3)_4]$ and $[Si(OSi(OH)_3)_4]$ clusters respectively, which can be considered as minimal models for TS-1 and silicalite, respectively.

As further improvement we present here results obtained on more realistic clusters (vide infra Figure 2a), hereafter named as Si-sil and Ti-sil, for mimicking silicalite and TS-1, respectively. Ti-sil and Si-sil have been obtained by cutting a fraction of the MFI framework around the T1 site.[15] This approach has the significant advantage to consider the structural strain induced on Ti(Si)−O−Si moieties by the cyclic structures surrounding them. The effect of zeolite framework constraint on the reactivity of Ti has been investigated on Ti−chabazite[16] and on TS-1[17] using a periodic (CRYSTAL[18]) and embedding (QMPOT[19]) approach, respectively. However, in such studies, the vibrational peculiarities have not been discussed.

Experimental Methods

To limit the computational demand, in our calculations, the cluster/embedded cluster ONIOM[20] scheme implemented in the Gaussian 98 code[21] has been adopted. Basically, in ONIOM, a portion of a large cluster (the real system R) can be defined as the model part M of the whole cluster (stick and balls in Figure 2): dangling bonds are saturated by H atoms (the so-called "link-atoms"). The final ONIOM energy (as such as gradients and so on) is defined as

$$E(\text{ONIOM}) = E(\text{HM}) + [E(\text{LR}) - E(\text{LM})] \qquad (1)$$

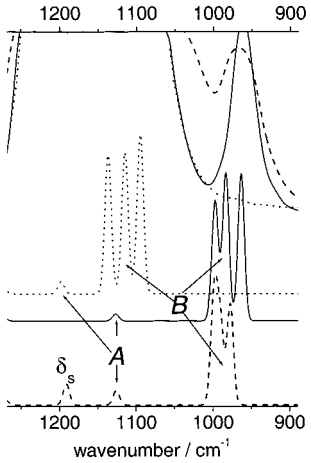

Figure 1. Comparison between experimental (top curves) and computed (bottom curves) IR spectra of dehydrated TS-1 (solid lines) and silicalite (dotted lines). Dashed line spectra refer to TS-1 in interaction with NH_3: experimental (upper curve) and computed (lower curve).

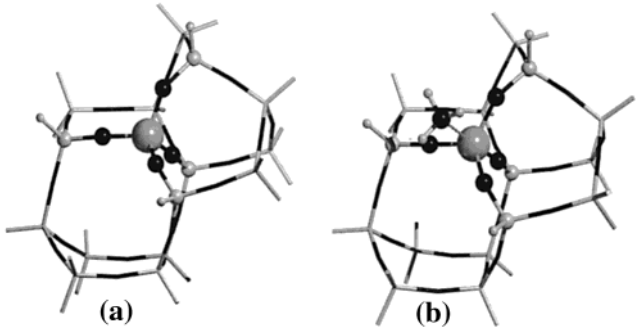

Figure 2. Clusters used in ONIOM calculations: atoms included in M zone are represented with stick and balls, while sticks refers to the remaining part of R. H link atoms are omitted. Part (a) optimized bare TS-1 model. Part (b) optimized TS-1/NH_3 model.

* Corresponding author. Tel +39011-6707841, fax +39011-6707855. E-mail: Lamberti@ch.unito.it.

10.1021/jp0257698 CCC: $22.00
Published on Web 06/25/2002

where E(LR) is the energy of the whole cluster calculated at (RHF/3-21G(H,N,Si,O), 3-21G*(Ti)) low (L) level, E(LM) is the M energy at (RHF/3-21G(H,N,Si,O), 3-21G*(Ti)), and E(HM) is the M energy obtained at (B3-LYP[22]/6-311+G(d,p)-(H,N,Si,O), ppp(Ti)) high (H) level. Here, ppp represents the basis-set employed for Ti atom: it is composed by effective small core pseudopotentials[23] + LANL2DZ[23] + Ahlrichs "p" polarization function.[24] A detailed description of the adopted ONIOM scheme has been reported elsewhere.[25]

For IR spectra, a Brucker IFS 66 FTIR spectrometer equipped with an HgCdTe cryodetector has been used. For all spectra, a resolution of 2 cm^{-1} has been adopted. Samples have been studied in transmission mode on thin self-supported wafers. NH_3 has been dosed in gas phase through a vacuum manifold directly connected with the measure cell.

Results and Discussion

In the totally siliceous cluster, the central $Si(OSi)_4$ moiety, exhibits four Si−O (Si−Si) distances in the 1.622−1.633 Å (3.113−3.242 Å) interval, and three narrow Si−O−Si angles (144.4°, 148.2° and 156.5°) and a large one at 171.5°. It is characterized by two main vibrational features: a single band centered at 1198 cm^{-1} and a triplet (1138, 1115, and 1095 cm^{-1}) labeled in Figure 1 as components A and B respectively. Band A (IR, weak) is the totally symmetric combination of the four ν_{asym}(Si−O−Si) modes while, feature B (IR, strong, triply degenerated in a perfect T_d symmetry), originates from their asymmetric combinations. The computed IR spectrum covers only a part of the broad experimental absorption due to the heterogeneity of T site environments in MFI (12 independent T sites), which is supposed to slightly affect the frequencies of A and B modes. The experimental spectrum can so be considered as the sum of 96 A and B features corresponding to the 96 T centers in the orthorhombic MFI unit cell.

Insertion of Ti in the central T site of the cluster strongly perturbs the geometrical features of the local structure. The optimized geometry of the $Ti(OSi)_4$ moiety agrees well with EXAFS data, being the four Ti−O distances in the 1.797−1.813 Å interval (to be compared with the experimental value: 1.79−1.81 ± 0.01 Å),[11,12] the four Ti−Si distance in the 3.306−3.426 Å range (experimental 3.26−3.38 ± 0.02 Å),[12] and the four Ti−O−Si angles divided into two narrower ones at 146.2° and 151.3° and two larger at 168.6° and 169.5° (experimental 143° ± 5° and with 162° ± 5°).[12] The higher shells are much less affected, being the average O−Si distance of the four adjacent O atoms increased by 8 10^{-3} Å and all the remaining distances perturbed by less than 10^{-3} Å, a difference that is far beyond the significance level of our calculations. Figure 2a reports the optimized geometry of the bare cluster. Coming to the vibrational features, Ti insertion significantly influences the B triplet, which is now located at 998, 984, and 964 cm^{-1}, i.e., in a region very close to the experimental component centered at 960 cm^{-1} (Figure 1). Also mode A undergoes a consistent red shift, moving to 1127 cm^{-1}. This band, not visible in the experimental IR spectrum since appearing in the broad 1250−1030 cm^{-1} range (where A and B features of the predominant siliceous part of TS-1 strongly absorb), corresponds to the 1125 cm^{-1} Raman band,[10] enhanced when UV laser is used.[13,14] Table 1 summarizes the computed and the experimental vibrational features.

The interaction of probe molecules with Ti(IV) centers in TS-1[9−11,26,27] has been widely used to prove the isomorphic insertion of Ti in the framework. The measurement of the modification induced on the different spectroscopic features of TS-1, by the distortion of the local geometry around Ti induced by the adsorption, gives relevant information on the interaction between probe molecules and the active site of the catalyst. A progressive blue shift of the 960 cm^{-1} band has been observed upon increasing the equilibrium pressure of H_2O, NH_3, and CH_3OH probe molecules.[9−11,14,26,27] In those works the 960 cm^{-1} band has been intuitively explained in terms of a mode with prevailing Si−O character perturbed by adjacent framework Ti center. According to this simple model, the interaction of Ti(IV) with an adsorbed molecule will imply a reduction of the perturbation induced on the adjacent Si−O moieties, resulting in the convergence of the 960 cm^{-1} band with the unperturbed ν_{asym}(Si−O−Si) mode adsorbing in the wide 1250−1030 cm^{-1} interval (Figure 1).

TABLE 1: Computed Vibrational Frequencies (A and B Modes) of Bare Si-sil and Ti-sil Clusters, Modeling Silicalite-1 and TS-1 Zeolites Respectively, and of the Engaged Ti-sil/NH_3 Cluster, Mimicking the Interaction of Ammonia with a Ti(IV) Site in TS-1[a]

system	A (cm^{-1})	$B\,\bar{\nu}_1$ (cm^{-1})	$B\,\bar{\nu}_2$ (cm^{-1})	$B\,\bar{\nu}_3$ (cm^{-1})	$B\,\langle\bar{\nu}\rangle$ (cm^{-1})
Si-sil	1198	1095	1115	1138	1115.0
Ti-sil	1127	964	984	998	980.9
Ti-sil/NH_3	1126	978	991	999	989.6
TS-1	1125 (Raman)				960 (IR)
TS-1+ NH_3					968 (IR)

[a] For sake of comparison also the centers of mass of the corresponding experimental IR or Raman features are reported, when available.

Our calculated frequencies on the Ti-sil/NH_3 complex (Figure 2b) reflect what was experimentally observed, namely the B triplet upward shifted to 999, 991, and 978 cm^{-1} (Figure 1 and Table 1). If comparison is made on the center of mass, it moves from 981 to 988 cm^{-1}, in agreement with the $\Delta\bar{\nu} = 8$ cm^{-1} experimentally observed. Concerning the A mode, the center of mass appears at the same frequency (1126 vs. 1127 cm^{-1}), being slightly intensified. Comparison with experimental shift is not feasible for IR data; it is however worth noticing that Raman experiments[14] did not show a significant shift of the A band upon water adsorption. The new band at 1191 cm^{-1} (Figure 1) is the δ_s umbrella mode of NH_3 upward shifted (from the computational value of 1000 cm^{-1}) upon absorption on the Ti center. The first shell rearrangements reproduce quite well EXAFS data obtained on TS-1 contacted with NH_3: indeed, from our calculations, the average Ti−O distance increment is +0.03 Å, to be compared with the experimental increment of +0.05 ± 0.03 Å.[26,27] It is, however, worth noticing that the experimental value reported in refs 26 and 27 refers to high NH_3 loading, where two NH_3 molecules are adsorbed per Ti center. Also, the second shells are slightly expanded: now the four Ti−Si distances lie in the 3.360−3.457 Å interval, assuming the two couples of Ti−O−Si angles values of 156.5°, 150.7° and 167.9°, 178.4°. Conversely the average O−Si distance of the four adjacent O atoms decreases to values more close to those observed on the Si-sil cluster. The Ti−N distance is 2.35 Å. Unfortunately no second shell EXAFS analysis has been reported up to now on the TS-1/NH_3 system. On the energetic ground, the calculated binding energy is 45.5 kJ mol^{-1}, reduced to 33.0 kJ mol^{-1} after correction of the basis set superposition error.[28] Such a value seems to be rather underestimated with respect to the 60 kJ mol^{-1} determined by microcalorimetry data;[26,27] however, comparison is hardly feasible because of the average nature of the calorimetric datum,[29] which reflects the heterogeneity of the real catalyst, containing both perfect [$Ti(OSi)_4$] and defective (hydrolyzed) [$TiOH(OSi)_3$] moieties together with defective [$SiOH(OSi)_3$] hydroxyl nests where NH_3 forms H-bonded adducts.[7,9,11,12,14,15,26,27] A computational study

on the hydrolyzed [$TiOH(OSi)_3$] site is in progress. Finally, it is finally worth noticing that the adopted cluster approach underestimates long range interactions (correctly reproduced only when periodic approaches are adopted) and that DFT based Hamiltonians cannot take into proper account dispersive forces. As far as the first point is concerned, a periodic approach is in progress on the Ti−chabazite system (Si/Ti = 11). To give an estimation of the fraction of the binding energy due to dispersive interactions, an MP2 Hamiltonian should be used. Note, however, that an MP2 study on this system is far from being trivial.

In conclusion, our computational approach is able to nicely explain the basic spectroscopic features of TS-1 and their perturbation upon absorption of probe molecules.

Acknowledgment. This project has been supported by MURST (Cofin 2000, Area 03): "*Structure and reactivity of catalytic centers in zeolitic materials*". We are indebted to P. Ugliengo and V. Bolis for fruitful critical discussion.

References and Notes

(1) Taramasso, M.; Perego, G.; Notari, B. U.S. Patent 4410501, 1983.

(2) Notari, B. *Adv. Catal.* **1996**, *41*, 253, and references therein.

(3) Hölderich, W.; Hesse, M.; Naümann, F. *Angew. Chem., Int. Ed. Engl.* **1988**, *27*, 226.

(4) Millini, R.; Previdi Massara, E.; Perego, G.; Bellussi, G. *J. Catal.* **1992**, *137*, 497.

(5) Lamberti, C.; Bordiga, S.; Zecchina, A.; Carati, A.; Fitch, A. N.; Artioli, G.; Petrini, G.; Salvalaggio, M.; Marra, G. L. *J. Catal.* **1999**, *183*, 222.

(6) Lamberti, C.; Bordiga, S.; Zecchina, A.; Artioli, G.; Marra, G.; Spanò, G. *J. Am. Chem. Soc.* **2001**, *123*, 2204.

(7) Pei, S.; Zajac, G. W.; Kaduk, J. A.; Faber, J.; Boyanov, B. I.; Duck, D.; Fazzini, D.; Morrison, T. I.; Yang, D. S. *Catal. Lett.* **1993**, *21*, 333.

(8) Lamberti, C.; Bordiga, S.; Zecchina, A.; Artioli, G.; Marra, G. L.; Spanò, G. *J. Am. Chem. Soc.* **2001**, *121*, 2204.

(9) Boccuti, M. R.; Rao, K. M.; Zecchina, A.; Leofanti, G.; Petrini, G. *Stud. Surf. Sci. Catal.* **1989**, *48*, 133.

(10) (a) Scarano, D.; Zecchina, A.; Bordiga, S.; Geobaldo, F.; Spoto, G.; Petrini, G.; Leofanti, G.; Padovan, M.; Tozzola, G. *J. Chem. Soc., Faraday Trans.* **1993**, *89*, 4123. (b) Deo, G.; Turek, A. M.; Wachs, I. E.; Huybrechts, D. R. C.; Jacobs, P. A. *Zeolites* **1993**, *13*, 365.

(11) (a) Bordiga, S.; Coluccia, S.; Lamberti, C.; Marchese, L.; Zecchina, A.; Boscherini, F.; Buffa, F.; Genoni, F.; Leofanti, G.; Petrini, G.; Vlaic, G. *J. Phys. Chem.* **1994**, *98*, 4125. (b) Blasco, T.; Camblor, M.; Corma, A.; Pérez-Parriente, J. *J. Am. Chem. Soc.* **1993**, *115*, 11806.

(12) Gleeson, D.; Sankar, G.; Catlow, C. R. A.; Thomas, J. M.; Spanó, G.; Bordiga, S.; Zecchina, A.; Lamberti, C. *Phys. Chem. Chem. Phys.* **2000**, *2*, 4812.

(13) Li, C.; Xiong, G.; Xin, Q.; Liu, J.; Ying, P.; Feng, Z.; Li, J.; Yang, W.; Wang, Y.; Wang, G.; Liu, X.; Lin, M.; Wang, X.; Min, E. *Angew. Chem., Int. Ed. Engl.* **1999**, *38*, 2220.

(14) Ricchiardi, G.; Damin, A.; Bordiga, S.; Lamberti, C.; Spanò, G.; Rivetti, F.; Zecchina, A. *J. Am. Chem. Soc.* **2001**, *123*, 11409.

(15) Bordiga, S.; Ugliengo, P.; Damin, A.; Lamberti, C.; Spoto, G.; Zecchina, A.; Spanò, G.; Buzzoni, R.; Dalloro, L.; Rivetti, F. *Top. Catal.* **2001**, *15*, 43.

(16) Zicovich-Wilson, C. M.; Dovesi, R.; Corma, A. *J. Phys. Chem. B* **1999**, *103*, 988.

(17) Ricchiardi, G.; de Man, A.; Sauer, J. *Phys. Chem. Chem. Phys.* **2000**, *2*, 2195.

(18) Dovesi, R.; Saunders: V. R.; Roetti, C.; Causà, M.; Harrison, N. M.; Orlando, R.; Aprà, E. *CRYSTAL 95 User documentation*; University of Torino: Torino, Italy, 1995.

(19) Eichler, U.; Brändle, M.; Sauer, J. *J. Phys. Chem. B* **1997**, *101*, 10035.

(20) Humbel, S.; Sieber, S.; Morokuma, K. *J. Chem. Phys.* **1996**, *105*, 1959.

(21) Frisch, M. J.; Trucks, G. W.; Schlegel, H. B.; Scuseria, G. E.; Robb, M. A.; Cheeseman, J. R.; Zakrzewski, V. G.; Montgomery, Jr., J. A.; Stratmann, R. E.; Burant, J. C.; Dapprich, S.; Millam, J. M.; Daniels, A. D.; Kudin, K. N.; Strain, M. C.; Farkas, O.; Tomasi, J.; Barone, V.; Cossi, M.; Cammi, R.; Mennucci, B.; Pomelli, C.; Adamo, C.; Clifford, S.; Ochterski, J.; Petersson, G. A.; Ayala, P. Y.; Cui, Q.; Morokuma, K.; Malick, D. K.; Rabuck, A. D.; Raghavachari, K.; Foresman, J. B.; Cioslowski, J.; Ortiz, J. V.; Baboul, A. G.; Stefanov, B. B.; Liu, G.; Liashenko, A.; Piskorz, P.; Komaromi, I.; Gomperts, R.; Martin, R. L.; Fox, D. J.; Keith, T.; Al-Laham, M. A.; Peng, C. Y.; Nanayakkara, A.; Gonzalez, C.; Challacombe, M.; Gill, P. M. W.; Johnson, B.; Chen, W.; Wong, M. W.; Andres, J. L.; Gonzalez, C.; Head-Gordon, M.; Replogle, E. S.; Pople, J. A. Gaussian 98, Revision A.7, Gaussian, Inc.: Pittsburgh, PA, 1998.

(22) (a) Lee, C.; Yang, W.; Parr, R. G. *Phys. Rev. B* **1988**, *37*, 785−789. (b) Becke, A. D. *J. Chem. Phys.* **1993**, *98*, 1372, 5628.

(23) Hay, P. J.; Wadt, W. R. *J. Chem. Phys.* **1985**, *82*, 299.

(24) Schaefer, A.; Huber, C.; Ahlrichs, R. *J. Chem. Phys.* **1994**, *100*, 5829.

(25) Damin, A.; Bordiga, S.; Zecchina, A.; Lamberti, C. *J. Chem. Phys.* **2002**, *117*, 226.

(26) Bolis, V.; Bordiga, S.; Lamberti, C.; Zecchina, A.; Petrini, G.; Rivetti F.; Spanò, G. *Langmuir* **1999**, *15*, 5753.

(27) Bolis, V.; Bordiga, S.; Lamberti, C.; Zecchina, A.; Petrini, G.; Rivetti F.; Spanò, G. *Microporous Mesoporous Mater.* **1999**, *30*, 67.

(28) Lendvay, G.; Mayer, I. *Chem. Phys. Lett.* **1998**, *297*, 365.

(29) The average nature of the calorimetric datum is opposite to the spectroscopic one that is specific for the Ti site.